ELSEVIER

Spectrochimica Acta Part A 55 (1999) 1471–1484

SPECTROCHIMICA ACTA PART A

Correlation between asymmetric and spherical top: imperfect quantum bifurcationsG + CB. Zhilinskii [a], I.N. Kozin [a,*], S. Petrov [b]

[a] *Laboratoire de Physico-Chimie de l'Atmosphère, Université du Littoral, MREID, 59140 Dunkerque, France*
[b] *Chemistry Department, Moscow State University, Moscow 119899, Russia*

Received 10 June 1998; accepted 20 November 1998

Abstract

The rotational energy level structures of quasi-spherical top molecules is investigated through the analysis of systems of stationary points on classical rotational energy surface. The series of simplest typical bifurcations of stationary points are given, as a quasi-spherical molecule evolves to the spherical top limit due to rotational excitation or molecular isotopomerisation. In this way the correlation between asymmetric and spherical top rotation energy multiplets is studied for A_4 and AB_4 molecules and corresponding isotopomers. It is demonstrated that the correlation depends on the point symmetry of the asymmetric top molecule. Slight symmetry breaking from C_{2v} point symmetry down to C_s results in the appearance of imperfect bifurcations [M. Golubitsky and D.G. Schaeffer, 'Singularities and Groups in Bifurcation Theory', vol. 1, Springer-Verlag, 1984]. The effect of imperfect bifurcation and its manifestation in molecular rotational spectra are discussed. © 1999 Elsevier Science B.V. All rights reserved.

Keywords: Rotational energy; Bifurcations; Point symmetry

1. Introduction

There are two main approaches in the theory of rotational spectra of non-linear molecules. The majority of molecules are treated with a more customary and traditional approach [1], while it is very effective to use the spherical tensor formalism in the treatment of spectra of spherical top molecules [2,3]. This is a semiclassical method where the invisible barrier separating highly symmetrical molecules from the rest disappears. The semiclassical method employs the concept of rotational energy surface which was extensively developed by Harter and Patterson [4,5]. Within this approach, the rotational spectrum and its properties are completely defined by the rotational energy surface. On the one hand, it allows an instructive insight into molecular dynamics and provides very elegant explanation to the observed groups of levels or level clusters in the spectrum [5,6]. On the other hand, it can also produce accurate quantitative results. It was demonstrated that it gives highly precise calculation of spectrum patterns based on the surface trajectories and the tunnelling paths [4]. Therefore the semiclassical

* Corresponding author. Present address: Mathematics Institute, University of Warwick, CV4 7AL Coventry, UK.
E-mail address: kozin@maths.warwick.ac.uk (I.N. Kozin)

1386-1425/99/$ - see front matter © 1999 Elsevier Science B.V. All rights reserved.
PII: S1386-1425(98)00331-X

methods supplies a common platform for the analysis or rotational spectra of all types of non-linear molecules.

Another interesting aspect of exploitation of rotational energy surface is an explanation of spectrum evolution under variation of parameter [7–9]. From the physical point of view the choice of the total angular momentum J as such a parameter, is the most natural one since it is an integral of motion and its variation is possible for an arbitrary molecule. The basic phenomenon which may appear under parameter variation is a bifurcation of a stationary point in the system of surface trajectories. Classical bifurcations of rotational energy surfaces with different symmetry were analysed and systematically described for pure rotational problems by Pavlichenkov and Zhilinskii [8,9] within the phenomenological approach similar to the classification by symmetry of second-order phase transitions in solid state physics [10]. The manifestation of quantum bifurcations was predicted and demonstrated in different quantum systems. The recent reviews are given in [11–14]. The sequences of bifurcations corresponding to consecutive transformation of the same stationary point were also predicted and observed in the rotational spectra [15–17]. More importantly for the present paper, it is possible to study the sequence of bifurcations in the correlation between rotational energy surfaces of asymmetric and spherical tops [18].

It is known that spectra of quasi-symmetrical and quasi-spherical molecules are especially rich on appearance of bifurcations. It is very attractive to consider a whole class of molecules with the same equilibrium configuration and potential but different nuclear masses. Provided that the initial molecule has high symmetry, an appropriate parameter for isotopical substitution will lift down the symmetry. Already having J as the first parameter, the study of the multi-parameter problem addresses the question, "what happens to the bifurcation upon lowering of symmetry?". The bifurcation may persist but the symmetry breaking generally results in a decrease of the number of allowed types of bifurcations. However if the symmetry violation is small, another phenomenon is possible. It is related to the so-called 'imperfect bifurcation' which is well known in the classical theory of bifurcations [19]. An imperfect bifurcation corresponds to the appearance of stationary points in the neighbourhood of another stationary point which does not change its stability. The imperfect bifurcation is usually related to more complicated bifurcation which takes place under the presence of higher symmetry [20,21].

In the present paper, we introduce necessary tools and consider the transformation of the rotational energy surface of a spherical top molecule down to asymmetric under the variation of the total angular momentum, J, and isotopical substitution. Special attention is given to the role of imperfect bifurcation. The multi-parameter problem is proposed and studied here using a simple phenomenological two-parameter model which is rich enough to reflect the relation between symmetrical bifurcations and less or non-symmetrical imperfect bifurcations. The model may be a prototype for the spectra of A_4 and AB_4 spherical top molecules, but it is hoped the analysis will be of more general use. As for the practical importance, the results may be used to predict spectrum features of isotopically substituted molecules.

2. Model

Let us consider a tetrahedral A_4 molecule. The isotopic substitution of four masses by:

$$m_1 = m_2 = m - \delta, \tag{1}$$

$$m_3 = m + \delta(1 + d), \tag{2}$$

$$m_4 = m + \delta(1 - d) \tag{3}$$

leads us to an $A_2A'A''$ molecule with C_s point symmetry. The prime or double prime over A-atom indicates slight isotopical modification, i.e. $\delta \ll m$. There are two particular cases in Eqs. (1)–(3): the case $d = 0$ is reduced to an $A_2A'_2$ molecule which has C_{2v} point group and the case $d = 2$ is related to an A_3A' molecule which has C_{3v} point group. For any $0 \leq d \leq 2$ the molecule is nearly spherical top, and as a result the orientation of the principal inertia moment axes depends strongly on d. We can choose the reference frame in such a way that its axes coincide with the

principal inertia axes of asymmetric top with $\delta > 0$, $d = 0$. Let x, y, and z axes be respectively the axes of intermediate, maximal, and minimal inertia momenta. This implies that the x axis coincides with one of S_4 axes of regular tetrahedron and y and z axes are orthogonal to the symmetry refection planes of the tetrahedron. If $d \neq 0$ the inertia tensor is non-diagonal in the chosen frame. Its elements are given by the following expressions supposing that all nuclei are located at the distance $r_{AA} = r_e$ from each other being in the corners of the regular tetrahedron:

$$I_{xx} = r_e^2 m - \frac{d^2\delta^2 r_e^2}{4m}, \tag{4}$$

$$I_{yy} = r_e^2 m - \frac{1}{2}\delta r_e^2 - \frac{\delta^2 r_e^2}{2m}, \tag{5}$$

$$I_{zz} = r_e^2 m + \frac{1}{2}\delta r_e^2 - \frac{\delta^2 r_e^2}{2m} - \frac{d^2\delta^2 r_e^2}{4m}, \tag{6}$$

$$I_{xz} = I_{yz} = 0, \tag{7}$$

$$I_{xy} = -\frac{\sqrt{2}}{4} d\delta r_e^2 \left(1 - \frac{\delta}{m}\right). \tag{8}$$

Any changes in the equilibrium geometry due to isotopical substitution are assumed to be negligible. After inversion of the inertia tensor matrix, the rigid rotor part of the rotational Hamiltonian takes the following form:

$$\hat{H}_{rr} = B_{xx}\hat{J}_x^2 + B_{yy}\hat{J}_y^2 + B_{zz}\hat{J}_z^2 + B_{xy}\hat{J}_x\hat{J}_y, \tag{9}$$

where $\hat{J}_i$ are the operators of projection of the total angular momentum in the molecular coordinate frame.

The rotational constants take simple expressions if we restrict ourselves with linear in δ/m terms:

$$B_{xx} = \frac{1}{2mr_e^2}, \tag{10}$$

$$B_{yy} = \frac{1}{2mr_e^2}\left(1 + \frac{\delta}{2m}\right), \tag{11}$$

$$B_{zz} = \frac{1}{2mr_e^2}\left(1 - \frac{\delta}{2m}\right), \tag{12}$$

$$B_{xy} = \frac{1}{2mr_e^2}\frac{\sqrt{2}d\delta}{2m}. \tag{13}$$

Therefore we can use the following phenomenological rotational Hamiltonian to characterise asymmetry of the mass distribution for the molecule $A_2A'A''$ with the equilibrium configuration being the regular tetrahedron:

$$\hat{H}_{rr} = B_{xx}\left[\hat{J}_x^2 + \left(1 + \frac{\delta}{2m}\right)\hat{J}_y^2 + \left(1 - \frac{\delta}{2m}\right)\hat{J}_z^2 - \frac{\sqrt{2}d\delta}{2m}\hat{J}_x\hat{J}_y\right]. \tag{14}$$

Note, that the Hamiltonian (Eq. (14)) becomes the standard symmetric top Hamiltonian when $d = 2$, through an appropriate rotation in the xy plane.

Similarly we can obtain the rigid rotor Hamiltonian for the isotopically substituted AB_4 molecule. However it has exactly the form (Eq. (14)) in the linear approximation in δ/m. The mass of the central nucleus A does not contribute to the approximate rotational constants (Eqs. (10)–(13)) since the displacement of the nucleus A from the centre of the mass is proportional to δ/m and consequently the central nucleus contributes to the rotational energy as the square of the small parameter. The rotational constants for the AB_4 molecule are not required for further discussion but the reader can easily obtain them using equality $r_{AA} = \sqrt{8/3}r_{AB}$ which comes from the geometrical consideration.

The centrifugal correction is independent of δ in the simplest approximation. We employ the centrifugal distortion term with tetrahedral symmetry which has maxima at C_{3v} axes and minima at S_4 axes of the regular tetrahedron. In the molecular frame introduced above it takes the form:

$$\hat{H}_{cd} = 4\hat{J}_x^4 + 3\hat{J}_y^4 + 3\hat{J}_x^4 + 4\hat{J}_x^2\hat{J}_y^2 + 10\hat{J}_y^2\hat{J}_z^2 + 4\hat{J}_z^2 + 4\hat{J}_z^2\hat{J}_x^2. \tag{15}$$

Both effects of the mass asymmetry and the centrifugal distortion can now be combined into one effective rotational Hamiltonian:

$$\hat{H}_{eff} = B_{xx}\left[\hat{J}^2 + \frac{\delta}{2m}(\hat{J}_y^2 - \hat{J}_z^2) + \frac{\delta}{2m}\sqrt{2}d\hat{J}_x\hat{J}_y\right] - t\hat{H}_{cd}. \tag{16}$$

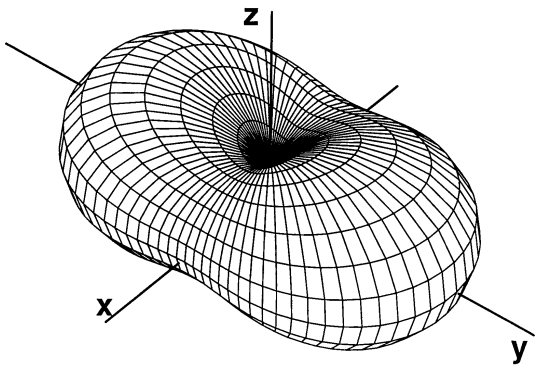

Fig. 1. Rotational energy surface for a rigid asymmetric top with the axes system orientated along the principal inertia axes. The axes y and z are stable precession axes while the axis x is unstable. For A_2A_2' and AB_2B_2' molecules the y and z axes correspond to the C_{2v} axes of the O_h group whereas the x axis corresponds to the C_{4v} axis.

It is important to remember here that we used the body-fixed coordinated system with axes coinciding with principal inertia axes of isotopically substituted molecule. This choice of axes being natural for an asymmetrical top leads to nonstandard axes orientation in the corresponding spherical top but it is quite convenient for the analysis of correlation between asymmetrical and spherical tops. In what follows we suggest that the reader consult Figs. 1 and 2 systematically for the choice of axes.

In this paper we explore classical tools for the study of the Hamiltonian (Eq. (16)). The classical

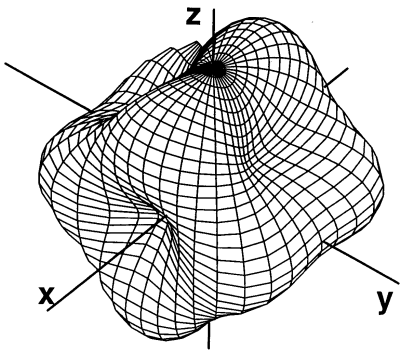

Fig. 2. Rotational energy surface for a spherical top molecule. It is the $R^{4(4,A_1)}$ invariant function with maxima in C_3 axis positions. The axes x, y and z are chosen so that they correspond to the principal inertia axes of the rotational energy surface in Fig. 1. The y and z axes are unstable precession axes while the x axis is stable.

Hamiltonian can be easily obtained through the substitution of the operators $\hat{J}_i$ by their classical analogies J_i. It is useful to introduce dimensionless normalised projections of the total angular momentum $j_x = J_x/J$, $j_y = J_y/J$ and $j_z = J_z/J$. Since the scaling of rotational Hamiltonian does not change the energy structure of rotational multiplet, our scaled classical effective Hamiltonian can be written as:

$$\tilde{H}_{\text{eff}} = \frac{1}{4} + \frac{1}{4}\frac{\delta}{m}[(j_y^2 - j_z^2) + \sqrt{2}dj_x j_y] - \frac{tJ^2}{B_{xx}} \times \left(j_x^4 + \frac{3}{4}j_y^4 + \frac{3}{4}j_z^4 + j_x^2 j_y^2 + \frac{5}{2}j_y^2 j_z^2 + j_z^2 j_x^2 \right), \tag{17}$$

where j_x, j_y, and j_z may be expressed as usual spherical angles:

$$j_x = \cos\varphi \sin\theta, \tag{18}$$

$$j_y = \sin\varphi \sin\theta, \tag{19}$$

$$j_z = \cos\theta. \tag{20}$$

The analysis of the Hamiltonian (Eq. (17)) reveals that the relative contributions of the rigid rotor and the centrifugal distortion terms can be effectively estimated by the parameter α:

$$\alpha = \arctan\left(\frac{2m}{\delta}\frac{tJ^2}{B_{xx}}\right). \tag{21}$$

It depends on the type of the molecule, the centrifugal distortion term and the J value. Typical values of B/t are of the 10^3–10^4 range. The isotopic substitution of H by D (e.g. in $CH_4 \rightarrow CH_2D_2$) gives $2m/\delta = 6$ whereas the substitution of ^{35}Cl by ^{37}Cl results in $2m/\delta = 72$. In the latter example α can be as high as 0.46π when $J = 10$–33. This is almost the upper limit for α.

We can finally express the Hamiltonian (Eq. (17)) in the form which depends on two meaningful parameters only:

$$H_{\text{eff}} = 1 + \frac{1}{4}\cos\alpha[(j_y^2 - j_z^2) + \sqrt{2}dj_x j_y - 2] - \sin\alpha \times \left(j_x^4 + \frac{3}{4}j_y^4 + \frac{3}{4}j_z^4 + j_x^2 j_y^2 + \frac{5}{2}j_y^2 j_z^2 + j_z^2 j_x^2 - \frac{1}{4} \right), \tag{22}$$

where a constant term has been added for the convenience of further analysis. The addition of a constant term, as well as scaling, does not modify the structure of the rotational multiplet. The sum in the Hamiltonian (Eq. (22)) consists of three terms. The first one is the constant which gives a base energy and is not important in the analysis. The second one is the rigid rotor term. It gives asymmetry of the rigid rotor due to inertia tensor. The third term is the spherical centrifugal distortion. The second and third terms have weights which are proportional to $\cos\alpha$ and $\sin\alpha$ correspondingly. It is obvious to see that there are two limiting cases. When $\alpha\sim 0$ the second term is dominant and we have the rigid rotor limit. When $\alpha\sim\pi/2$ the third term is leading and we obtain the spherical top limit. Varying α from 0 to $\pi/2$ the model (Eq. (22)) is tuned from one limit to another. Both parameters α and d are dimensionless. The physically allowed variation of d is limited by a set of discrete values due the number of possible isotopes. It should be thought of as a small integer or rational number.

3. Rotational energy surface and orbifold representation

The internal energy level structure of rotational multiplet in the case of relatively high J values can be easily understood in terms of classical rotational energy surface [4,5,22]. The rotational energy surface represents the rotational energy as a function of direction of the total angular momentum vector with respect to the molecular frame. Generally the topology of the system of trajectories on the rotational energy surface can vary with the absolute value of J. In the rigid asymmetric top limit ($\alpha\sim 0$) the rotational energy surface has a well-known shape of three-axially deformed sphere (see Fig. 1). In the other limit ($\alpha\sim\pi/2$) the centrifugal distortion effects become preponderant and the mass asymmetry is negligible. The corresponding rotational energy surface is shown in Fig. 2. It is important to note that the coordinate frame is the same on both figures and the frame orientation is held fixed throughout the paper.

The rotational energy surfaces in two limiting cases have different systems of stationary points. There are six stationary points for the asymmetric rigid rotor and 26 stationary points for the spherical top. When $d=0$, six stationary points of the asymmetric top keep their positions in the molecular-fixed frame as α increases, but their stability nevertheless changes. It is the subject of this paper to study the transformation from one limit to another and we shall refer to it as a 'correlation'. Particularly the variation of α from 0 to $\pi/2$ keeping $d=0$ exemplifies the $A_2A_2'\leftrightarrow A_4$ and $AB_2B_2'\leftrightarrow AB_4$ correlations. Another special case of $d=2$ gives $A_3A'\leftrightarrow A_4$ and $AB_3B'\leftrightarrow AB_4$ correlations.

If we allow for d to be nonzero ($d\neq 2$) the situation changes qualitatively. Then in the $\alpha\sim 0$ limit the rotational energy surface has also six stationary points but their location in the molecular frame depends on the d parameter of the Hamiltonian (Eq. (22)). The increase of the centrifugal distortion term now produces two effects. The first one is similar to the previous case: it is the modification of the number of stationary points. New stationary points should arise during the variation of α. The second effect is due to the change of positions of the stationary points on the rotational energy surface. Two stationary points situated on the z axis are fixed, but another four undergo a shift as the centrifugal distortion increases. Therefore the variation of α gives in general case $A_2A_2'A''\leftrightarrow A_4$ and $AB_2B'B''\leftrightarrow AB_4$ correlations.

The knowledge of stationary point system provides a complete characteristic of rotational energy surface. Consequently all correlations must be investigated from the point of view of bifurcation sequence of stationary points. To represent the correlations we use two types of diagrams. First we construct an energy bifurcation diagram which shows the evolution of the energies of stationary points as a function of the control parameter. The energy diagrams were widely used earlier in many publications concerning qualitative analysis of ro-vibrational energy level structure [18,22–24]. They can be almost immediately related to the corresponding quantum energy spectrum.

The energy diagram gives no precise information about positions of stationary points. It is however instructive to study the position change as well. To this end, one needs the graphical representation of the phase space of the rotational energy surface. Since the rotational energy surface has a symmetry, there is no necessity to represent the whole phase space but only one point of each set formed by the symmetry group operations on this point. Such a set is called 'group orbit' and the phase space of group orbits forms 'orbifold'. In other words, an orbifold consists of points, each of which represents a group orbit. It is quite natural to distinguish the points in the orbifold by the symmetry operations which do not alter the position of the point in the phase space. These symmetry operations form the subgroup of the molecular symmetry group, and the name of the subgroup can be used as a label for the group orbit. We call the subgroup a 'stabiliser' in this context. Generally, the higher the symmetry of the stabiliser, the lower the multiplicity of group orbit. For instance, for the rotational energy surface given by Fig. 2 the stationary points of minimal energy have C_{4v} symmetry and 6-fold multiplicity while the stationary points of maximal energy have C_{3v} symmetry and 8-fold multiplicity.

The group orbits with the same stabiliser can be unified into one 'stratum' [25]. Since our phase space is a two-dimensional sphere S_2, a stratum can be just a set of points (zero-dimensional stratum), a part of a curve (on-dimensional stratum), or a part of surface (two-dimensional stratum). Group orbit isolated within its stratum is called 'critical orbit' [25]. Particularly zero-dimensional stratum, which consists of one or several critical orbits. Critical orbits always correspond to an extrema of any smooth function given on the phase space. This knowledge of critical orbits immediately provides us with the information about corresponding extrema on the rotational energy surface though an extremum is not necessarily a critical orbit.

The schematic representation of the orbifold was used in a number of previous works [16,26–28] to show the evolution of the system of stationary points. Below we represent orbifolds using 'invariant polynomials' as coordinates rather than the spherical angles (Eqs. (18)–(20)). An advantage of invariant coordinates is that their symmetry is as high as the symmetry of the Hamiltonian itself, i.e. they are invariant under the action of the given symmetry group. Generally the Hamiltonian can be either expressed or expanded in the series of invariant polynomials. There exist main and auxiliary invariant polynomials which all form the 'integrity basis' [22,25,29–31].

The actual symmetry of the Hamiltonian (Eq. (22)) depends on the parameter values but it is always higher than the point symmetry of the molecule because of the time reversal symmetry. The latter results in the inversion symmetry of the **J**-vector in the molecular coordinate system. Consequently the total symmetry of the Hamiltonian (Eq. (22)) is O_h rather than T_d for the tetrahedral molecules A_4 and AB_4, D_{2h} for $A_2A'_2$ and $AB_2B'_2$ molecules which have C_{2v} point symmetry and C_{2h} for $A_2A'A''$ and $AB_2B'B''$ molecules which have only C_s symmetry. Since our model (Eq. (22)) does not distinguish if there is a central atom or not we can make the discussion below more general when speaking about correlation between the Hamiltonians with different symmetry, rather than between molecules. We adopt the following notations for molecular correlations: $D_{2h} \leftrightarrow O_h$ and $C_{2h} \leftrightarrow O_h$, since they make molecular and Hamiltonian symmetry more obvious. There is yet another reason for this. These correlations can be viewed as a simple possible scenario of bifurcation sequences on the rotational energy surface of quasi-spherical molecule with D_{2h}, or C_{2h} symmetry, respectively. One should however distinguish this kind of correlation from the traditional correlation tables between symmetry operations of point groups (see [32]).

The orbifolds for three different groups O_h, D_{2h} and C_{2h} are required. We construct all invariant polynomials from normalised projections of the total angular momentum j_x, j_y and j_z [25,31], taking into account the apparent restriction $j_x^2 + j_y^2 + j_z^2 = 1$. For the O_h group they can be expressed in the classical limit in terms of two main invariant polynomials of the fourth and sixth order as $\theta_1 = j_x^4 + j_y^4 + j_z^4$ and $\theta_2 = j_x^2 j_y^2 j_z^2$. The new coordinates can be used to represent orbits of O_h group action on the phase space which is S_2

Table 1
Strata for the O_h group action on S_2[a]

Stabiliser	Critical orbit	Region of the orbifold
C_{4v}	Yes	$\theta_1=1,\ \theta_2=0$
C_{3v}	Yes	$\theta_1=1/3,\ \theta_2=1/27$
C_{2v}	Yes	$\theta_1=1/2,\ \theta_2=0$
C_s	No	$1/2<\theta_1<1,\ \theta_2=0$
C'_s	No	$\theta_1=1-2s+3s^2/2$ $\theta_2=s^2(1-s)/4$ $0<s<1,\ s\neq 2/3$
C_1	No	Internal points

[a] Basic invariant polynomials $\theta_1=j_x^4+j_y^4+j_z^4$ and $\theta_2=j_x^2j_y^2j_z^2$ are used as coordinates for the orbifold representation.

sphere. The orbifold for the natural action of the O_h group on S_2 and strata equations in terms of invariant polynomials are given in Fig. 10 of Ref. [33], and Table 1 of this paper, respectively. For the D_{2h} group action on the S_2 sphere there are two basic polynomial invariants of the second order in j_x, j_y, and j_z components. They can be defined as $\theta_a=j_x^2-j_y^2$ and $\theta_b=j_z^2$. The strata equations in terms of invariant polynomials are given in Table 2. The representation of the space of orbits in polynomial coordinates for the C_{2h} point group is slightly more complicated. This is due to the fact that the integrity basis constructed from invariant polynomials includes now two main polynomials and one auxiliary polynomial. According to the general theory [22] in such a case, to distinguish the orbits one needs the values of two main polynomials and the sign of one auxiliary polynomial. The main polynomials can be chosen as in the D_{2h} case and the auxiliary polynomial $\varphi=j_xj_y$. The strata equations are given in Table 3.

Table 2
Strata for the D_{2h} group action on S_2[a]

Stabiliser	Critical orbit	Region of the orbifold
C_{2v}^z	Yes	$\theta_a=1,\ \theta_b=0$
C_{2v}^y	Yes	$\theta_a=0,\ \theta_b=-1$
C_{2v}^x	Yes	$\theta_1=0,\ \theta_b=1$
C_s^{xy}	No	$\theta_a=0,\ -1<\theta_b<1$
C_s^{yz}	No	$0<\theta_a=\theta_b+1<1$
C_s^{xz}	No	$0<\theta_a=-\theta_b+1<1$
C_1	No	Internal points

[a] Basic invariant polynomials $\theta_a=j_z^2$ and $\theta_b=j_x^2-j_y^2$ are used as coordinates for the orbifold representation.

Table 3
Strata for the C_{2h} group action on S_2[a]

Stabiliser	Critical orbit	Region of the orbifold
C_2^z	Yes	$\theta_a=1,\ \theta_b=0,\ \varphi=0$
C_s^{xy}	No	$\theta_a=0,\ -1\leq\theta_b\leq 1$ $-1/2<\varphi<1/2$
C_1	No	Internal points

[a] Two basic invariant polynomials $\theta_a=j_z^2$ and $\theta_b=j_x^2-j_y^2$ and one auxiliary invariant polynomial $\varphi=j_xj_y$ are needed to represent unambiguously all group orbits. Only the sign of the auxiliary polynomial is important.

4. Correlation analysis

4.1. $D_{2h}\leftrightarrow O_h$ correlation

General features of the $D_{2h}\leftrightarrow O_h$ diagram can be found from the comparison of the action of O_h and D_{2h} groups on the sphere. It should be noted that the correlation depends on the choice of the axes orientation of the D_{2h} subgroup with respect to the O_h group. In fact there are two nonequivalent D_{2h} subgroups of the O_h group depending on the axes orientation. We follow the choice introduced in Section 2 with three C_{2v} axes of the D_{2h} group coinciding with one C_{4v} and two C_{2v} axes of the O_h group (see Figs. 1 and 2). In order to formulate some consequences about the evolution of the system of stationary points along the correlation diagram we need to know the list of critical orbits for the O_h and D_{2h} groups and their correlation.

The minimal set points of the D_{2h} invariant function includes six points (three two-point critical orbits). These six points have a fixed position in the phase space along the whole correlation diagram. On the other hand, the O_h invariant function has 26 stationary points (one 6-point orbit, one 8-point orbit, and one 12-point orbit). When the O_h symmetry breaks down to D_{2h} with the axes orientation as described above, the O_h orbits are split correspondingly into D_{2h} orbits. For example, one C_{3v} invariant 8-point orbit is

split into two different 4-point orbits of the D_{2h} group and so on. The complete correlation between group orbits of the O_h and D_{2h} groups is given in Table 4.

The representation of the space of orbits of the D_{2h} group's action on the two-dimensional sphere is given in Fig. 3. Critical orbits in the rigid rotor limit are given as empty circles. There are three of them since they are two-point orbits. Along the correlation diagram three critical orbits must be transformed into seven: three two-point, three four-point, and one eight-point. This can be done through different sequences of bifurcations which depend on the particular form of the Hamiltonian. But the minimal number of elementary bifurcations needed for that is four. The correlation diagram shown in Fig. 4 gives a particular example of such a bifurcation sequence. It corresponds to the Hamiltonian (Eq. (22)) with d set to zero. The evolution of critical orbits is shown as solid lines in the figure. Since critical orbits always correspond to extrema they give us part of the stationary points. The energies of other stationary points are given by dotted lines (one-dimensional orbits) and dashed lines (two-dimensional orbits). Orbit stabilisers with respect to the D_{2h} group are indicated together with multiplicity. On the right hand side of Fig. 4, the stabilisers of O_h critical orbits are shown in the $\alpha = 0$ limit.

Table 4
Correlation between group orbits of O_h, D_{2h}, and C_{2h} symmetry groups

O_h	D_{2h}	C_{2h}
C_{4v} (6 points)	C_{2v} (2 points) C_s (4 points)	C_s (2 points) C_1 (4 points)
C_{3v} (8 points)	C'_s (4 points) C''_s (4 points)	C_1 (4 points) 2[C_s] (2+2 points)
C_{2v} (12 points)	C'_{2v} (2 points) C''_{2v} (2 points) C_1 (8 points)	C_2 (2 points) C_s (2 points) 2[C_1] (4+4 points)
C_s (24 points)	$C_s+C'_s$ (4+4 points) 2[C_1] (8+8 points)	2[C_1] 4[C_1]
C'_s (24 points)	2[C_s] (4+4 points) 2[C_1] (8+8 points)	2[C_1] 4[C_1]
C_1 (48 points)	6[C_1]	12[C_1]

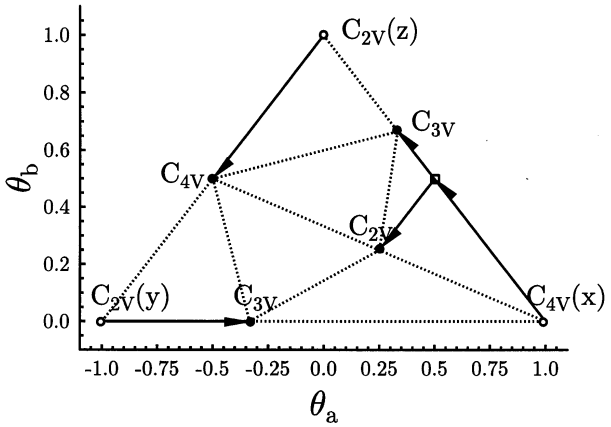

Fig. 3. Orbifold of the D_{2h} group action in S_2 is presented in the space of two invariant polynomials $\theta_a = j_x^2 - j_y^2$ and $\theta_b = j_z^2$. Empty circles indicate the critical orbits, square denotes a bifurcation. Filled circles show the orbits of stationary points at the spherical top limit ($\alpha = \pi/2$). Dashed lines show the stratification due to the action of the O_h group. Solid lines display the dynamic of the orbits of stationary points as α varies from 0 to $\pi/2$ in the Hamiltonian (Eq. (22)) with $d = 0$. Note that the symmetry of all axes is given with respect to the O_h group.

In order to represent in detail the system of stationary points, we can split the whole variation range of α into four subintervals. The first bifurcation occurs at $\alpha = \arctan(1/4) \approx 0.24$ [34]. Thus for $\alpha < \arctan(1/4)$ the system of stationary points includes only critical orbits, i.e. the points along the symmetry axes: the rotational energy surface has two maxima at the y axis, two minima at the z axis and two saddle points at the x axis. The point $\alpha = \arctan(1/4)$ corresponds to the bifurcation of the unstable stationary point at the x axis. The x axis becomes a stable axis of rotation and two new unstable stationary axes arise. Their positions undergo a shift in the xz plane as α increases further. The lines with arrows in Fig. 3 show as the new stationary points move upon the increase of α. Ten stationary points exist in the region $\arctan(1/4) < \alpha < \arctan(1/2) \approx 0.46$. When α reaches $\arctan(1/2)$ two simultaneous bifurcations occur. Both y and z axes become unstable and new stable axes appear. Similarly to the first bifurcation, the new axes move in the xy, and yz planes, respectively,

(see Figs. 3 and 4). There are 18 stationary points on the rotational energy surface in the region $\arctan(1/2) < \alpha < \pi/4$. Finally, the new stable axis in the xz plane bifurcates at $\alpha = \pi/4$. For $\alpha > \pi/4$ this orbit again becomes stable, whereas unstable stationary points arise which correspond to the orbit in the two-dimensional stratum. The last bifurcation is denoted as a square in Fig. 3. In total we have two local bifurcations with C_2 broken symmetry and two non-local bifurcations with C_2 and C_s broken symmetry. The notation of bifurcations is explained in more details in Refs. [18,26]. The dotted lines in Fig. 3 show stratification due to O_h group. If the D_{2h} orbifold were folded along them we would get the orbifold of O_h group (cf. Fig. 10 of [33]). That is why the limiting positions of the stationary points in Fig. 3 are strictly defined.

4.2. $C_{2h} \leftrightarrow O_h$ correlation

The energy correlation diagram for the model (Eq. (22)) with $d = 1$ is presented in Fig. 5. The orbifold representation is given in Fig. 6 and it shows the positions of stationary points in the rigid rotor limit as empty circles. It is seen that x and y axes are not critical orbits any longer. The principal difference between D_{2h} and C_{2h} symmetry groups is the presence of the single critical orbit: z-axis. It displays the same type of behaviour as the similar critical orbit in the case of the D_{2h} symmetry group: the bifurcation with the C_2 broken symmetry. Two other critical orbits of the D_{2h} symmetry group become non-critical C_s symmetry orbits in the C_{2h} group and the corresponding stationary points are shifted in the xy plane. Due to this they cannot change their stability without breaking C_s symmetry and instead of two bifurcations at y and x axes with C_2 broken symmetry, as in the case of the D_{2h} symmetry, we have now one bifurcation with C_s broken symmetry and one C_1 type fold in the xy plane. The C_1 bifurcation occurs on the set of C_s symmetrical orbits. The last bifurcation shown in Fig. 6 is a generic C_1 type fold which results in the simultaneous appearance of four equivalent maxima and four saddle points. Its prototype in the D_{2h} system is the bifurcation at $\alpha = \pi/4$. The bifurcations are indicated as squares in Fig. 6.

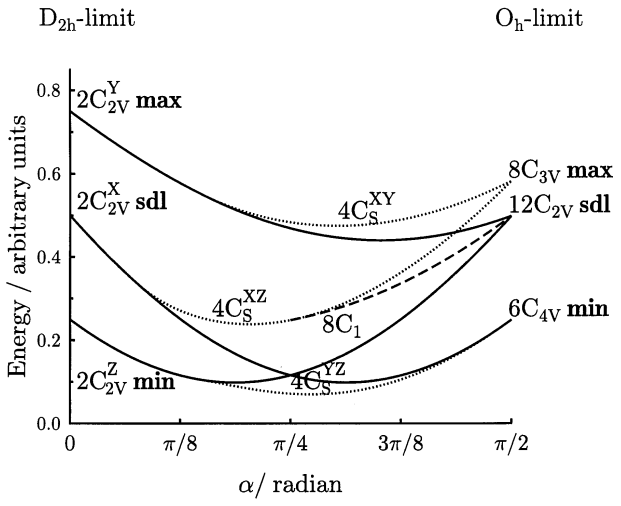

Fig. 4. Energy correlation diagram between asymmetric top (D_{2h} symmetry) and spherical top (O_h symmetry) for the Hamiltonian (Eq. (22)) with $d = 0$. Solid lines represent energy of D_{2h} critical orbits, dotted lines show energy of stationary points which belong to orbits in one-dimensional strata and dashed line indicates energy of stationary points which belong to orbits in two-dimensional stratum. Multiplicity of orbits is indicated as an integer number before symmetry label.

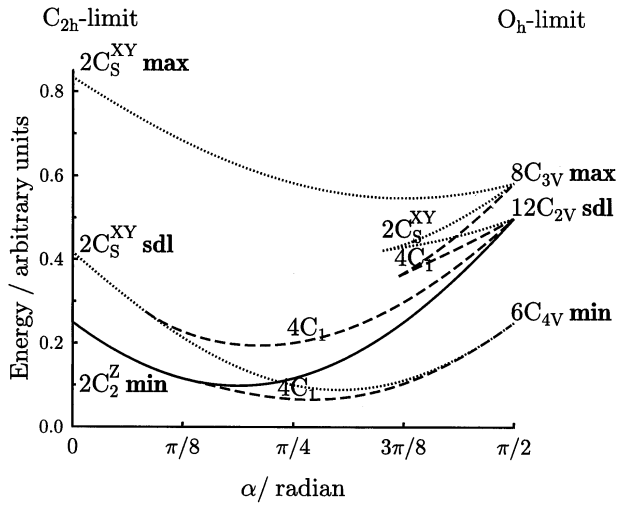

Fig. 5. Energy correlation diagram between asymmetric top (C_{2h} symmetry) and spherical top (O_h symmetry) for the case of $d = 1$ in the model (Eq. (22)). Solid line represents energy of C_{2h} critical orbit, dotted lines show energy of stationary points which belong to orbits in one-dimensional stratum and dashed lines indicate energy of stationary points which belong to orbits in two-dimensional stratum. Multiplicity of orbits is indicated as an integer number before symmetry label.

Again, the limit positions of stationary points at $\alpha = \pi/2$ are pre-defined because of the tetrahedral symmetry. The general comparison of the energy correlation diagrams in Figs. 4 and 5 reveals that low energy parts look similar. But relatively small isotopic substitution affects rather strongly the high energy part of the diagrams.

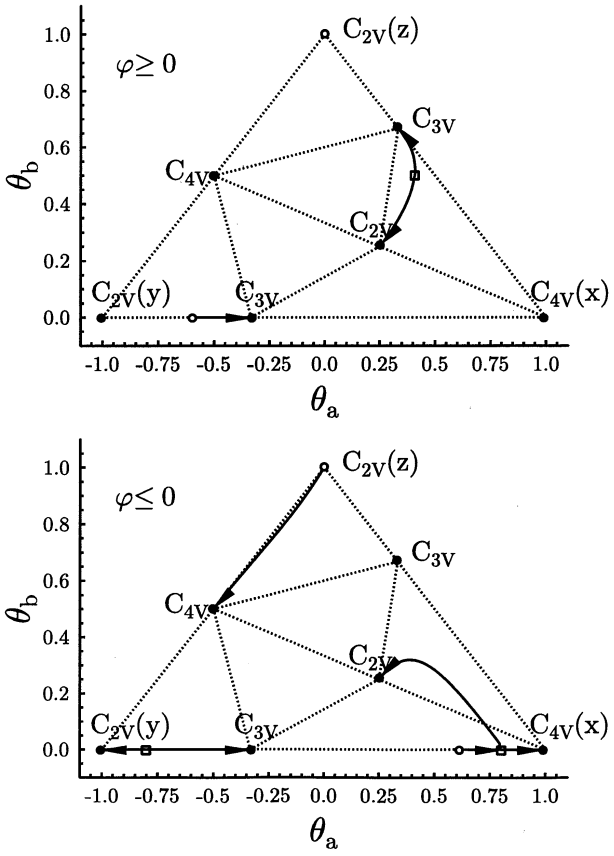

Fig. 6. Orbifold of the C_{2h} group action in S_2 is presented in the space of two invariant polynomials $\theta_a = j_x^2 - j_y^2$ and $\theta_b = j_z^2$ together with the sign of the auxiliary invariant $\varphi = j_x j_y$. Empty circles indicate the orbits of stationary points at $\alpha = 0$ for the Hamiltonian (Eq. (22)) with $d = 1$, while filled circles show the orbits of stationary points at the spherical top limit ($\alpha = \pi/2$). Squares denote bifurcations. Dashed lines show the stratification due to the action of the O_h group. Solid lines display the dynamic of the stationary points as α varies from 0 to $\pi/2$. Points with $\varphi = 0$ in two graphs (left and right sides of big triangles) should be glued together. Note that the symmetry of all axes is given with respect to the O_h group.

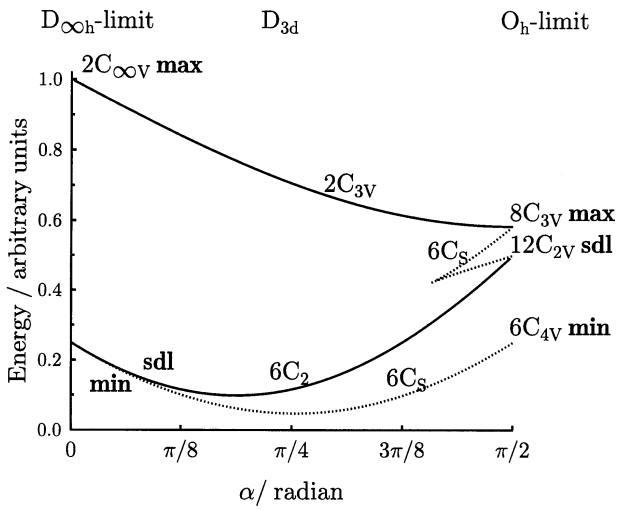

Fig. 7. Energy correlation diagram between rigid symmetric top ($D_{\infty h}$ symmetry), nonrigid symmetric top (D_{3d} symmetry) and spherical top (O_h symmetry). It corresponds to the case of $d = 2$ in the model (Eq. (22)). Solid lines represent energy of D_{3d} critical orbits and dotted lines show energy of stationary points which belong to orbits in one-dimensional stratum. Multiplicity of orbits is indicated as an integer number before symmetry label.

4.3. $D_{\infty h} \leftrightarrow D_{3d} \leftrightarrow O_h$ correlation

Finally it is easy and straightforward to obtain the correlation between symmetrical and spherical top molecules. The corresponding energy diagram is presented in Fig. 7 which is a natural evolution of the series given by Figs. 4 and 5. It is calculated by setting the parameter $d = 2$ in the Hamiltonian (Eq. (22)). Then the point symmetry of the equilibrium configuration of AA_3' and ABB_3' molecules is C_{3v}, but the symmetry of the rotational Hamiltonian is D_{3d}. Furthermore, in the absence of the centrifugal distortion ($\alpha = 0$) the Hamiltonian has yet higher symmetry which is apparently $D_{\infty h}$. Comparing Fig. 7 with Fig. 5 we see that the $D_{\infty h} \leftrightarrow D_{3d} \leftrightarrow O_h$ correlation is formed through the degeneracy of pairs of corresponding branches in the $C_{2h} \leftrightarrow O_h$ energy correlation diagram. Simultaneously two bifurcations at small values of α become one bifurcation at $\alpha = 0$. The phenomenon at $\alpha = 0$ corresponds to the bifurcation of the circular degenerate orbit located in the plane which is orthogonal to the C_{3v} symmetry axis. There is however no such bifurcation in the

correlation of the generic D_{3d} Hamiltonian since six saddle points and six minima become non-degenerate as in the case at any $0 < \alpha \leq \pi/2$. Six equivalent saddle points form one critical orbit of D_{3d} group with C_2 local symmetry while six minima form one non-critical orbit with C_s local symmetry. Another bifurcation is a non-local phenomenon consisting of six equivalent bifurcations in the symmetry planes of D_{3d} group [9].

5. Discussion

It is very well known that the topology of trajectories of the total angular momentum on the rotational energy surface, defines the rotation energy level structure of the J-multiplet [4,5]. Provided that the density of levels is sufficiently high, the wavefunctions of eigenstates with energy close to minima or maxima of the rotational energy surface, may be found as localised in the phase space adjacent to the corresponding minima or maxima of the rotational energy surface. The saddle points separate the regions of localisation. Therefore equivalent by symmetry, minima or maxima result in the appearance of quasi-degenerate quantum states [4–6]. In Fig. 4, the region of small α is analogous to the widely discussed spectrum of asymmetric rigid rotor [1,4]: the spectrum consists of two series of quasi-degenerate doublets of levels. One series of doublets originates in the wavefunctions localised around two symmetrical minima on the rotational energy surface while another one comes from two symmetrical maxima. However at higher values of α there occurs the first deviation from it due to the bifurcation at $\alpha = \arctan(1/4)$. Because of two new symmetrical minima on the x-axis, the new band of doublets appears. Two next bifurcations at $\alpha = \arctan(1/2)$ make further complications in the spectrum, bringing 4-fold minimum and maximum. As a result, two additional bands of quasi-degenerate quadruplets can be formed at low- and high-energy ends of the J-multiplet. Finally, at the point of last bifurcation, $\alpha = \pi/4$ the tetrahedral centrifugal distortion term, becomes comparable with rigid rotor asymmetry since $tJ^2 = B_{xx}\delta/2m$. The domination of the centrifugal term may lead to the third series of 4-fold clusters because of the appearance of 8-fold saddle point in the general stratum. In the O_h limit there is strictly only two bands: a series of 8-fold clusters of levels at high energy and 6-fold clusters at low energy of the J-multiplet.

The analysis of the rotational energy surface for $A_2A'A''$ and $AB_2B'B''$ molecules with the help of Fig. 5 shows that qualitatively their energy level structures should be similar to A_2A_2' or AB_2B_2' correspondingly, at small centrifugal distortion. Upon the increase of α the first bifurcation occurs at close value as above, but its type is different. The effect on the energy spectrum is the same though, the appearance of quasi-degenerate doublets. The second bifurcation in Fig. 5 has also its analogue in Fig. 4. It can result in 4-fold quasi-degeneracy of levels. This degeneracy is the highest strictly possible for C_{2h}. Two next bifurcations are imperfect ones as we will see below. There may be a series of doublets due to the bifurcation in the xy-plane and a series of quadruplets due to the bifurcation in the general stratum. Further formation of 6- or 8-fold clusters of levels due to the domination of the tetrahedral centrifugal distortion term is 'accidental' within C_{2h} symmetry but these clusters become native in the spherical top limit.

The comparison of two correlation diagrams between asymmetric and spherical top molecules upon isotopic substitution, reveals a qualitative difference between Hamiltonians with D_{2h} and C_{2h} symmetries. The difference is clearly seen in the classical limit when any violation of D_{2h} symmetry results in the modification of the type of observed bifurcations. We saw that in some cases when D_{2h} symmetry breaks, non-symmetrical bifurcation occurs in the neighbourhood of original D_{2h} symmetrical bifurcation (see Fig. 8). This phenomenon is known in the bifurcation theory as imperfect bifurcation [19]. Its characteristic signature is the so-called perturbed 'pitchfork' in the plane of stationary point position versus parameter. Fig. 9 shows the j_x coordinate of stationary points for a twice isotopically substituted molecule with $d = 0.03$, as α changes from 0 to $\pi/2$. This is not a real case since d is too small but it makes the perturbed pitchfork more obvious.

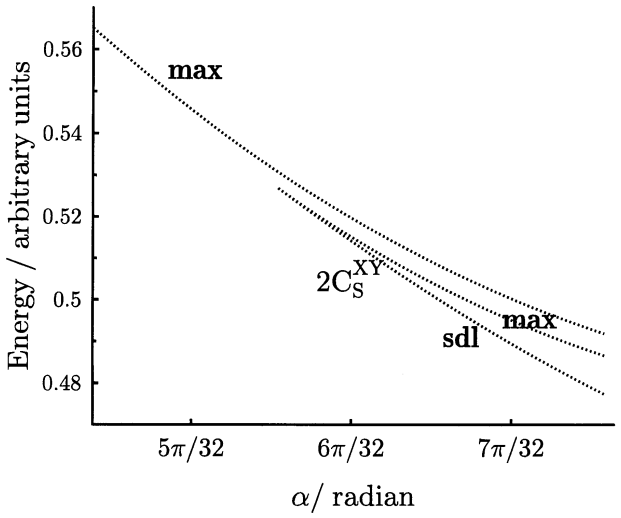

Fig. 8. Part of the energy correlation diagram between asymmetric top (C_{2h} symmetry) and spherical top (O_h symmetry) for the case of $d=0.03$ in the model (Eq. (22)). Dotted lines represent energy of stationary points which belong to orbits in one dimensional stratum.

When the perturbation is zero and two new maxima are identical (the case of D_{2h} symmetry) the pitchfork is symmetrical (cf. Fig. 9 of the present paper and Figs. 1.1 and 1.3 of Ref. [19]). For any small d, the old maximum evolves with α without changing its stability and the newly appeared one is different and nonsymmetric. This is immediately reflected in the energy difference of these stationary points which is evident from the energy correlation diagram given in Fig. 8.

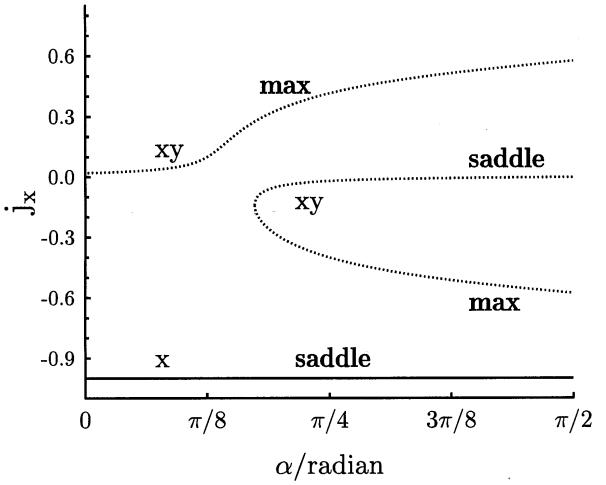

Fig. 9. Easy recognisable pitchfork of the bifurcation in the xy plane for the model (Eq. (22)) with parameter $d=0.03$. The ordinate is the normalised projection of the angular momentum on the x axis $j_x=J_x/J$.

It is very interesting to look at the imperfect bifurcation from the point of view of the reduction of the asymmetric top Hamiltonian. There is a common practice to use reduced effective rotational Hamiltonians. These Hamiltonians are D_{2h} invariant even for totally non-symmetric molecules. Particularly to get the reduced Hamiltonian form for the $A_2A'A''$ molecule we need to introduce the main axes system first. This will eliminate the $\hat{J}_x\hat{J}_y$ term but brings $\hat{J}_x^3\hat{J}_y$, $\hat{J}_x\hat{J}_y^3$, and $\hat{J}_x\hat{J}_y\hat{J}_z^2$ terms. The traditional procedure for elimination of these latter terms uses the method of contact transformations [1,35]. Although nonsymmetrical—with respect to the D_{2h} group—terms are allowed, the traditional reduced Hamiltonian consists of only D_{2h} symmetrical terms, and as a result we will raise the symmetry of the system and the imperfect bifurcation (if present) turns itself into symmetrical one: the pitchfork in Fig. 9 will become 'un-broken'. Consequently, the energy diagram on Fig. 8 will also be changed to the symmetrical form as in Fig. 4. This however violates the physical nature of the bifurcation.

The situation is 2-fold: on the one hand, the asymmetrical perturbation might be small enough to be detected in the quantum system because of the low level density. Indeed even assuming uniform level density the energy difference between extrema on the rotational energy surface should be rather big, since the expected degeneracy of levels is very high. This is completely analogous to a double-well potential with a central hump. When it is much lower than the first vibrational level, the energy level structure will be only slightly perturbed. The qualitative changes in the level structure are obvious when the perturbation is comparable with the typical level spacings. Therefore the energy perturbation due to isotopic substitution must be sufficiently big to allow the manifestation of the imperfect bifurcation in the quantum system and to make it separable from the symmetrical one. On the other hand, the near symmetrical or near spherical cases are always the subject of special considerations. A special pertur-

bation treatment for the reduction procedure is required when approaching the spherical top limit. Otherwise the perturbation series will be divergent since contact transformation operators (s-operators) are inversely proportional to δ/m which is assumed to be the small parameter here. The solution to this would be a non-standard form of reduced Hamiltonian which preserves the imperfect bifurcation.

The effect of imperfect bifurcation could be illustrated in another example. It is known that some AB_2 molecules can exhibit a bifurcation of the stable precession axis, which has the minimal inertia moment and is located in the molecular plane [36–38]. The molecule has C_{2v} symmetry and its rotational Hamiltonian in an isolated vibrational state has D_{2h} symmetry. There may be a case when not only the AB_2 molecule, but also the isotopically substituted molecule ABB′ has the bifurcation. If the mass variation is relatively small compared with the nuclear mass itself then the bifurcation in the ABB′ molecule can be in the close region of the phase space and at comparable value to the total angular momentum J as for AB_2. But the ABB′ molecule and its rotational energy surface have C_s, and C_{2h} symmetry, respectively. Therefore it must be an imperfect bifurcation. The manifestation of this effect also depends on the level density and the magnitude of asymmetrical perturbation as discussed above.

A similar analysis can be applied to the molecular systems which are close to the spherical top limit through isotopic substitution or accidentally: Sb_4, Ar_4 [39,40], CCl_4 [18], $FClO_3$ [41] and alike. Obviously, to predict qualitatively the presence or absence of bifurcations and particularly the imperfect bifurcation, more centrifugal distortion terms have to be taken into account. The given analysis provides however, the general recipe and the tools for considering such systems. It is believed that the presented model demonstrates all the main features which can be expected in the rotational spectrum of an isolated vibrational state of a quasi-spherical molecule. It is also hoped that it provides the useful insight and unified view on the spectra of asymmetric, symmetric and spherical top molecules. More complicated cases of interacting states are left beyond the scope of the present paper as they require another model and a separate study.

Acknowledgements

I.N.K. is indebted to CIES for the PECO fellowship. The work of S.P. was supported by the Russian Fund for Fundamental Investigations through the grant N 97-03-33622a.

References

[1] D. Papoušek, M.R. Aliev, Molecular Vibrational–Rotational Spectra, Elsevier, Amsterdam, 1982.
[2] L.C. Biedenharn, J.D. Louck, Angular Momentum in Quantum Physics, in: G.-C. Rota (Ed.), Encyclopaedia of Mathematics and Its Applications, Addison-Wesley, Reading, MA, 1981.
[3] R.N. Zare, Angular Momentum, Wiley, New York, 1988.
[4] W.G. Harter, C.W. Patterson, J. Chem. Phys. 80 (1984) 4241.
[5] W.G. Harter, Comp. Phys. Rep. 8 (1988) 319.
[6] A.J. Dorney, J.K.G. Watson, J. Mol. Spectrosc. 42 (1972) 135.
[7] W.G. Harter, C.W. Patterson, J. Math. Phys. 20 (1979) 1453.
[8] B.I. Zhilinskii, I.M. Pavlichenkov, Sov. Phys. JETP 65 (1987) 221.
[9] I.M. Pavlichenkov, B.I. Zhilinskii, Ann. Phys. 184 (1988) 1.
[10] L.D. Landau, E.M. Lifshitz, Statistical Physics, Pergamon, Oxford, 1965.
[11] I.M. Pavlichenkov, Phys. Report. 226 (1993) 175.
[12] B.I. Zhilinskii, Spectrochim. Acta Part A 52 (1996) 881.
[13] M.E. Kellman, Annu. Rev. Phys. Chem. 46 (1995) 395.
[14] T. Uzer, Phys. Rev. A 42 (1990) 5787.
[15] B.I. Zhilinskii, Lecture Notes in Physics, vol. 382, 487–489 (1991).
[16] G. Pierre, D.A. Sadovskii, B.I. Zhilinskii, Europhys. Lett. 10 (1989) 409.
[17] O.I. Davarashvili, B.I. Zhilinskii, V.M. Krivtsun, D.A. Sadovskii, E.P. Snegirev, Pis'ma ZhETF, 51, (1990) 17 [JETP Lett, 51 (1990) 18].
[18] I.M. Pavlichenkov, B.I. Zhilinskii, Chem. Phys. 100 (1985) 339.
[19] M. Golubitsky, D.G. Schaeffer, Singularities and Groups in Bifurcation Theory, vol. 1, Springer-Verlag, Berlin, 1984.
[20] R. Gilmore, Catastrophe theory for scientists and engineers, Wiley, New York, 1981.
[21] V.I. Arnol'd, A.N. Varchenko, S.M. Gusein-Zade, Singularity Theory, Nauka, Moscow, 1982.

[22] B.I. Zhilinskii, Theory of Complex Molecular Spectra [in Russian], Moscow University Press, Moscow, 1989.
[23] D.A. Sadovskii, B.I. Zhilinskii, J.-P. Champion, G. Pierre, J. Chem. Phys. 92 (1990) 1523.
[24] V.M. Krivtsun, D.A. Sadovskii, B.I. Zhilinskii, J. Mol. Spectrosc. 139 (1990) 126.
[25] L. Michel, Rev. Mod. Phys. 52 (1980) 617.
[26] D.A. Sadovskii, B.I. Zhilinskii, Phys. Rev. A 47 (1993) 2653.
[27] D.A. Sadovskii, B.I. Zhilinskii, L. Michel, Phys. Rev. A 53 (1996) 4064.
[28] B.I. Zhilinskii, S. Brodersen, M. Madsen, J. Mol. Spectrosc. 160 (1993) 192.
[29] W. Burnside, Theory of Groups of Finite Order, Cambridge, 1911.
[30] H. Weyl, The classical groups, their invariants and representations, Princeton University, New Jersey, 1939.
[31] M.V. Jarić, L. Michel, R.T. Sharp, J. Phys. 45 (1984) 1.
[32] P.R. Bunker, Molecular Symmetry and Spectroscopy, Academic Press, London, 1979.
[33] L. Michel, B.I. Zhinlinskii, (1997) preprint (IHES/P/97/54).
[34] S. Petrov, B.I. Zhilinskii, Opt. Spektrosk. (USSR) 81 (1996) 737.
[35] J.K.G. Watson, in: J.R. Durig (Ed.), Vibrational Spectra and Structure, vol. 6, Elsevier, New York, 1977, p. 1.
[36] B.I. Zhilinskii, I.M. Pavlichenkov, Opt. Spectrosc. (USSR) 64 (1988) 413.
[37] J. Makarewicz, J. Pyka, Mol. Phys. 68 (1989) 107.
[38] I.N. Kozin, I.M. Pavlichenkov, J. Chem. Phys. 104 (1996) 4105.
[39] L.L. Lohr, Int. J. Quant. Chem. 57 (1996) 707.
[40] L.L. Lohr, Mol. Phys. 91 (1997) 1097.
[41] F. Meguellati, G. Graner, K. Burczyk, H. Bürger, J. Mol. Spectrosc. 185 (1997) 392.